ELSEVIER

Polymer 44 (2003) 2911–2918

polymer

www.elsevier.com/locate/polymer

Phase morphology and melt viscoelastic properties in blends of ethylene/vinyl acetate copolymer and metallocene-catalysed linear polyethylene

J. Peón[a], J.F. Vega[a], B. Del Amo[b], J. Martínez-Salazar[a,*]

[a]*GIDEM, Instituto de Estructura de la Materia, CSIC, Serrano 113-123, 28006 Madrid, Spain*
[b]*Repsol-YPF I + D, Embajadores, 183, 28045 Madrid, Spain*

Received 5 July 2002; received in revised form 24 December 2002; accepted 20 February 2003

Abstract

The aim of this study was to determine the linear viscoelastic properties of a series of ethylene/vinyl acetate copolymer/metallocene-catalysed polyethylene (mPEs) blends. Newtonian viscosity showed a pronounced positive deviation from the double reptation model, which assumes miscibility or, at least, cooperative relaxation between the mixed species. Enhanced values of steady-state compliance and elastic indices with respect to those of the pure components were also noted. These features are typical of emulsion-like polymer blends and are thought to arise from additional relaxation processes associated with dispersed phase deformability. Application of the Palierne model for emulsions of two viscoelastic liquids showed good agreement with our experimental dynamic results at both ends of the phase diagram. However, the model failed at intermediate compositions. Through the application of several rheological criteria we were able to locate the phase inversion concentration at a weight fraction of $w = 0.60$ in the mPEs. It is suspected that, in this composition range, a fully co-continuous phase develops due to the phase inversion mechanism, which has considerable effects on the viscoelastic properties of the blends.

Keywords: Viscoelasticity; PE/EVA; Blends

1. Introduction

Despite the interest generated in the patent literature [1], to date, the rheological properties of ethylene/vinyl acetate copolymer (EVAc)/polyethylene (PE) blends have been scarcely investigated [2]. We recently observed certain characteristic features in the viscoelastic response of EVAc/low density polyethylene (LDPE) blends that point to these blends being heterogeneous polymeric systems [3].

In rheology, three phase behaviour patterns are generally considered for: (i) miscible single-phase systems, (ii) rather ill defined intermediate systems near the phase separation region, and (iii) immiscible two-phase systems [4,5]. It is very difficult to establish the miscibility of a blend in the melt state. The linear viscoelastic response obtained in small strain dynamic flow is an appropriate method of obtaining information on the homogeneity of polymer blends. Miscibility or homogeneity is generally assumed when the linear viscoelastic response of a blend can be expressed as a simple blending rule applied to the relaxation spectra of its base polymers. Moreover, the blending rules developed for homologous polymer blends are frequently valid for miscible blends. In the case of immiscible blends, the situation is more complex. The properties and rheology of immiscible blends are strongly dependent on morphology and, therefore, on the viscoelastic properties of the phases, mixing conditions and composition [5]. The more general case is the emulsion-like morphology, with a continuous phase (matrix) and a relaxed spherical dispersed phase. For this particular case, the mathematical models developed have attained a high degree of sophistication and take into account the viscoelastic nature of the phases, their deformability and hydrodynamic interaction between the particles of the dispersed phase.

The Palierne model [6] for emulsions of viscoelastic fluids has been proved to be highly efficient in describing the

* Corresponding author. GIDEM, Instituto de Estructura de la Materia, CSIC, Serrano 113-123, 28006 Madrid, Spain. Tel.: +34-915-616-800x3114; fax: +34-915-855-413.
E-mail address: jmsalazar@iem.cfmac.csic.es (J. Martínez-Salazar).

0032-3861/03/$ - see front matter © 2003 Elsevier Science Ltd. All rights reserved.
doi:10.1016/S0032-3861(03)00176-9

linear viscoelastic response of immiscible blends of flexible polymers [7–14]. The main feature of these systems is a characteristic increase in the values of the storage modulus G' at low frequencies, related to the deformation relaxation mechanism of the dispersed spherical particles and the interfacial tension between the phases. For a heterogeneous blend of two viscoelastic fluids, one can define various parameters associated with the system's morphology [15]. λ_M is a relaxation time for the blend; λ_P is the relaxation time associated with the deformation mechanism of the phases and λ_D is the terminal relaxation time of the blend. G_P is a characteristic secondary plateau modulus that appears at low frequencies associated with the dispersed morphology. All these variables strongly depend on the interfacial tension α, the particle radius R, and the linear viscoelastic features of the pure components, mainly the Newtonian viscosity ratio $K = \eta_{0,d}/\eta_{0,m}$, and relaxation time ratio $\chi = \tau_d/\tau_m$, between dispersed and continuous (matrix) phases.

The Palierne model expresses the complex modulus of the immiscible blend with a monodisperse droplet size distribution as

$$G^*(\omega) = G^*_m(\omega)\frac{1 + 3\phi H(\omega)}{1 - 2\phi H(\omega)} \tag{1}$$

with $H_i(\omega)$ given by

$$H(\omega) = \frac{4\left(\frac{\alpha}{R}\right)[2G^*_m + 5G^*_d] + [G^*_d - G^*_m][16G^*_m + 19G^*_d]}{40\left(\frac{\alpha}{R}\right)[G^*_m + G^*_d] + [2G^*_d + 3G^*_m][16G^*_m + 19G^*_d]} \tag{2}$$

G^*_d and G^*_m are the complex moduli of the dispersed phase and the matrix, respectively, α, the interfacial tension, ϕ, the volume fraction of the disperse phase, and R the particle radius. These expressions have been validated for the polydispersity of a droplet size distribution less than 2.3 [15]. This model's general formulation also contains the variables related to the interface $\beta'(\omega)$ and $\beta''(\omega)$, which take into account the viscoelastic properties of the interface (usually set at zero). It should be noted that the model includes no empirical variables and one can predict the linear viscoelastic response of an immiscible blend from measurable physical properties. If the interfacial tension α is unknown, the model can be used to determine its values by fitting experimental data.

Here we report a study performed on blends of a branched EVAc and a linear metallocene-catalysed PE (mPE) with moderate polydispersity indices. The rheological properties of these materials have been recently investigated [16,17]. Our primary focus was the linear rheological behaviour of these polymer blends in oscillatory shear. Morphology is very difficult to visualize because of the lack of contrast between the two polymers in the melt state. One could perform morphological studies in the solid state, but the morphology in this case might have nothing to do with that existing in the melt state due to co-crystallization or segregation effects during solidification of the material. Thus, we made use of rheological results derived from the melt to infer phase behaviour by applying current approaches that explain the behaviour of heterogeneous binary systems.

2. Experimental section

2.1. Materials and blend preparation

mPE and EVAc samples were supplied by Repsol-YPF, Spain. The properties of the polymers are presented in Table 1. Please refer to other works for details of the characterisation methods used [16,17]. Blending was carried out in an internal mixer Brabender Plasticorder fitted with a cam type rotor. The temperature was set at 160 °C and the torque at 15 N m. Mixing was continued for about 5 min until the torque and speed rotor reached stable values. The blends were assigned the abbreviation mPEw, w being the weight fraction of the mPE. The mixed mass was compression moulded for 2 min at 160 °C in a Schwabenthan Polystat 200T at a nominal pressure of 150 bar, and then quenched at room temperature. Disk specimens 25 mm in diameter were stamped for dynamic torsion measurements. The thickness of the compression-moulded samples was adjusted to around 0.5 mm, which is appropriate for rheological measurements. The pure materials were treated in the same conditions.

2.2. Melt rheology

Storage G' and loss G'' modulus measurements were performed in a stress controlled Bohlin CVO torsion rheometer, with parallel plates and cone-plate geometries of 25 mm diameter. This measurement was made at a maximum strain of 15% and was within the linear range for all the samples examined. The angular frequency dependence of the viscoelastic functions storage modulus G', loss modulus G'' and complex viscosity η^* were determined in the range 10^{-3}–10^2 rad s^{-1} from 130 to 190 °C. Determinations were repeated several times to minimise blending shear history and degradation effects. Time–temperature superposition was applied to frequencies and moduli [18] at the different temperatures. It was observed that the shift factors a_T and b_T

Table 1
Characterisation of the materials analysed: vinyl acetate content, melt flow index, weight average molecular weight, polydispersity index and branching content

Sample	VAc (%)	M_w	M_w/M_n	SCB < 6 C	LCB > 6 C
mPE	–	≈180,000	≈2.0	0.0	0.0
EVAc	27.0	911,00	3.9	5.5	<0.5

followed a simple Arrhenius-type expression for pure polymers. The values of E_{ah} were 5.4 kcal mol^{-1} for mPE and 15.5 kcal mol^{-1} for EVAc, in good agreement with recent reports [16,17]. For EVAc, a vertical shift had to be applied and the E_{av} value of 2.8 kcal mol^{-1} obtained corresponds to branched, thermorheologically complex ethylene based polymers [18]. The blends also fulfilled the time–temperature superposition principle. As shown in Table 2, the flow activation energy is reduced as the mPE content increases. The results of the superposition are omitted for the sake of brevity and since they provide no additional information on possible miscibility or immiscibility of the blends [3,19]. Only the results obtained at 160 °C are presented.

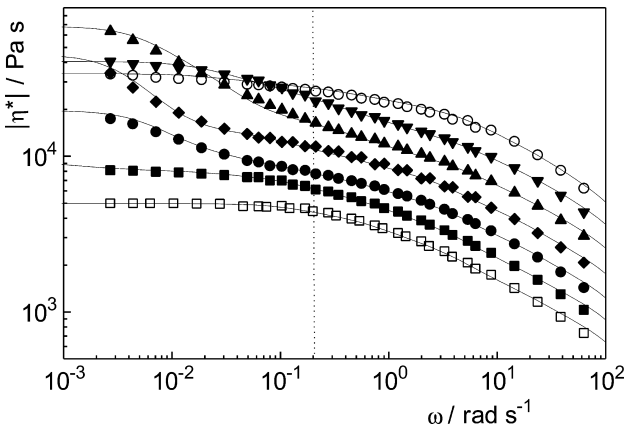

Fig. 1. Modulus of complex viscosity η^* versus angular frequency ω at 160 °C for the pure materials and some of the blends: (□) EVAc, (■) mPE020, (●) mPE040, (◆) mPE050, (▲) mPE060 (▼) mPE080 and (○) mPE. The lines corresponds to the spectral decomposition of the viscoelastic response fitted to the Maxwell model (see text).

3. Results and discussion

3.1. Dynamic viscoelastic measurements

First we considered the complex viscosity of the blends. Fig. 1 indicates characteristic behaviour at frequencies below 10^{-1} rad s^{-1} for the blends. A clear inflexion occurs in the complex viscosity curve of the blends as the weight fraction of the mPE, w, increases. Moreover, higher viscosity values than those corresponding to mPE are obtained for the blends with weight fractions higher than $w = 0.50$. This result resembles the typical yield stress response observed in viscosity η versus shear rate $\dot{\gamma}$ flow curves for structured liquids [4]. Nevertheless, in the case of linear viscoelastic measurements, the appearance of the yield stress-like curve cannot be related to the rupture or formation of inter-particle linkages, since the structure is largely unaffected over the linear viscoelastic response range. In this type of measurement, yield stress-like behaviour is associated with the presence of an interface [7–14]. The storage moduli G' of the blends at 160 °C are shown in Fig. 2. One can also clearly observe the enhanced elastic character of the blends, mainly for high w values. In the frequency range below 1 rad s^{-1}, the differences between blends and pure components become evident.

Fig. 3 shows a plot of $|\eta^*|$, at different levels of $|G^*|$, against blend composition. As it was pointed out by Utracki [5] the most suitable compositional plot to study the effect of blend composition is the Newtonian viscosity plot. However, values of viscosity obtained at constant shear stress could be used should be the unattainable Newtonian range [5]. Hence, we have selected the values of $|\eta^*|$ at constant $|G^*|$ (directly related to complex shear stress, $\sigma^* = G^*\gamma$) due to the impossibility to reach experimentally the terminal zone in the materials and samples studied. Before going into the details provided by the immiscibility models it is instructive to explore how much our experimental results differ from the most commonly used model of coupling two polymer components. Consequently, the double reptation model, which assumes miscibility between blend components, has been applied considering that both have the same entanglement modulus, G_N^0, similar melt density, ρ, and that the measured dynamic moduli in the terminal region are much smaller than G_N^0 in the range of frequencies studied. The equations for G' and G'' can then be expressed as a

Table 2
Rheological variables at 160 °C of the materials and blends examined. Newtonian viscosity η_0, steady-state compliance J_e^0 and relaxation time λ, and flow activation energies

Sample	η_0 (Pa s)	J_e^0 (Pa^{-1})	λ (s)	E_R	G_x (Pa)	E_{ah} (kcal mol^{-1})	E_{av} (kcal mol^{-1})
EVAc	4970	3.6×10^{-4}	1.8	0.35	55,000	15.5	2.8
mPE010	6350	5.6×10^{-4}	3.6	0.41	66,000	15.0	2.5
mPE020	8370	6.9×10^{-4}	6.1	0.47	82,000	16.1	3.5
mPE030	11,570	7.5×10^{-4}	18	0.62	84,000	13.2	4.9
mPE040	17,425	3.8×10^{-3}	73	0.68	88,000	10.1	0.6
mPE050	453,70	8.1×10^{-3}	630	0.86	12,2000	10.1	0.9
mPE060	743,95	4.1×10^{-3}	420	1.5	16,4000	8.0	2.1
mPE070	424,00	1.3×10^{-3}	64	0.95	16,7000	11.7	1.2
mPE080	422,75	9.6×10^{-4}	43	0.44	20,5000	6.4	1.4
mPE090	393,00	9.8×10^{-4}	40	0.35	23,5000	7.1	1
mPE	33,700	2.1×10^{-4}	8.0	0.25	25,0000	5.4	0.4

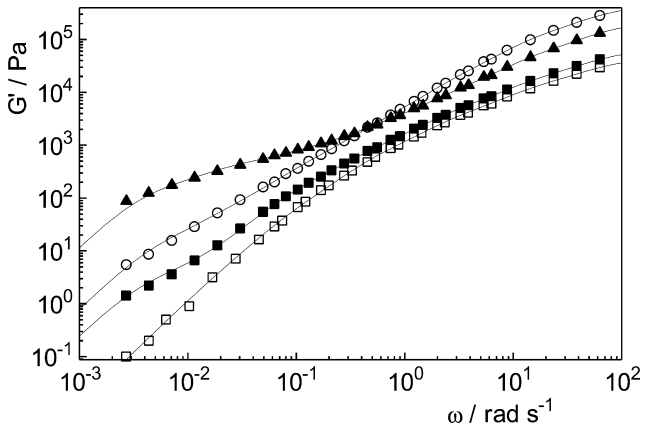

Fig. 2. Storage modulus G' versus angular frequency ω at 160 °C for the pure materials and some of the blends. See Fig. 1 legend for the description of the symbols and lines.

function of the pure-component properties [20]

$$G'(\omega) \cong \sum_{i=1}^{n}\sum_{j=1}^{n} w_i w_j \left[\frac{1}{4}(G_i'(\omega)^{-1/2} + G_j'(\omega)^{-1/2})^2\right]^{-1} \quad (3)$$

$$G''(\omega) \cong 2\sum_{i=1}^{n}\sum_{j=1}^{n} w_i w_j \left(\frac{1}{G_i''(\omega)} + \frac{1}{G_j''(\omega)}\right)^{-1} \quad (4)$$

From the calculated values of G' and G'', the values of $|\eta^*|$ at the different values of $|G^*|$ can be obtained. The experimental values of $|\eta^*|$ obtained at low values of $|G^*|$ show intense positive deviation from the double reptation model (see Refs. [3,20,21]) for blends with high values of w. This enhancement observed at low G^* values can be understood if we consider the emulsion model for the blends [5,7–14]. However, while operating at moderate to high values of G^* (moderate to high values of frequency, ω), a slight negative deviation from the model is observed for low values of w. An anomalous negative deviation in the compositional dependence of the viscosity function is a characteristic feature of immiscible blends in the non-linear regime [22–24]. This experimental feature is thought to be the consequence of an interfacial slip due to large deformations. Brochard and co-workers [25] suggest that in the interfacial region between two immiscible polymers, the chains are less entangled and form a region of lower viscosity and are thus able to slip at large deformations. However, the present results were obtained in the linear viscoelastic zone, where blend structure remains unaltered and slippage should not occur. At this point in the discussion, it should be considered that for low values of w there is no good transfer of the applied deformation across the interphase, when the majority blend component is that of lowest viscosity (EVAc). Fig. 3 also shows that the intermediate composition $w = 0.5$ seems to be a critical value; negative deviation from the miscible model becoming apparently below this characteristic composition. One can also regard it as a non-equilibrium blend morphology due to effects from the blending and sample preparation methods. However, we have found that the rheological measurements performed in successive frequency sweeps with the same sample were reliable in the whole range of frequencies studied, indicating neither morphological nor structural (degradation) changes exist.

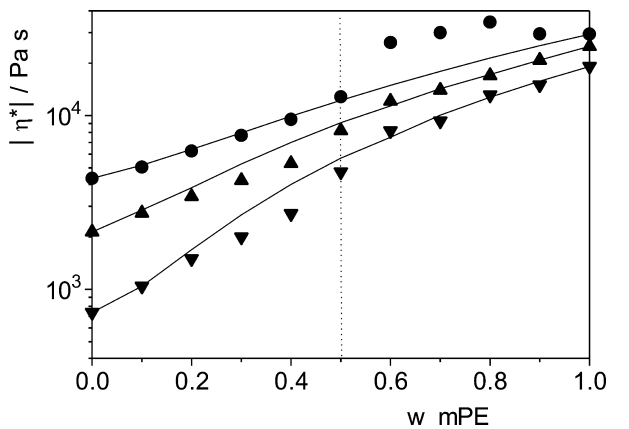

Fig. 3. Compositional dependence of viscosity at 160 °C for the blends: (●) $|\eta^*|$ ($|G^*| = 10^3$ Pa), (▲) $|\eta^*|$ ($|G^*| = 10^4$ Pa) and (▼) $|\eta^*|$ ($|G^*| = 4\times10^4$ Pa). Continuous lines represent the prediction of the miscible double reptation model.

Let us now analyse the terminal variables of the blends and pure materials examined. We have described the rheological linear viscoelastic data obtained by means of the generalised Maxwell model. This model was also used to calculate the characteristic variables of the terminal zone, as previously shown elsewhere (see Table 2) [3,16]. Table 2 lists the values of zero-shear viscosity η_0, steady-state compliance J_e^0 and terminal relaxation time λ defined as follows

$$\eta_0 = \lim_{\omega\to0}\left(\frac{G''(\omega)}{\omega}\right) \quad (5)$$

$$J_e^0 = \frac{1}{\eta_0^2}\lim_{\omega\to0}\frac{G'}{\omega^2} \quad (6)$$

$$\lambda = \lim_{\omega\to0}\frac{G'}{\omega G''} = \eta_0 J_e^0 \quad (7)$$

It may be noted that the values of η_0 are much enhanced at intermediate compositions. Also notice that the values of J_e^0 and λ (see Table 2) show strong positive deviation and maximum values at these intermediate compositions. The compositional variation of η_0 in immiscible systems has frequently been analysed using simple emulsion models [20,26]. The one proposed by Oldroyd is perhaps the most commonly applied [27]. This model coincides with the monodisperse Palierne's model given by Eqs. (1) and (2) in the terminal zone. Expanding the monodisperse Palierne's model at low frequencies in powers of ϕ one can obtain that the viscosity of a dilute emulsion of two incompressible and

totally immiscible Newtonian fluids is given by

$$\eta_0 = \eta_{0,m}\left[1 + \phi\frac{5K+2}{2(K+1)} + \phi^2\frac{(5K+2)^2}{10(K+1)^2}\right] \quad (8)$$

where ϕ is the volume fraction of the dispersed phase, $\eta_{0,m}$ is the viscosity of the matrix liquid and $K = \eta_{0,d}/\eta_{0,m}$, $\eta_{0,d}$ being the viscosity of the dispersed droplets. This dilute emulsion model is commonly used to predict the viscosity in the terminal zone on both sides of the phase diagram. We considered the weight w and volume ϕ fractions to be equal, i.e. it is assumed that both components have the same melt density ρ. In our case, $K = 0.15$ for high values of w and $K = 6.7$ for low values of w, assuming that the mixtures are completely immiscible. Similar increases in the extrapolated values of the terminal zone of the viscosity, η_0, than those predicted by the Oldroyd model can be observed in Fig. 4. However, the model does not serve to explain behaviour at intermediate compositions since pronounced deviations are not accounted for and the model is only valid for dilute emulsions.

In Fig. 5, we present the experimental G' values obtained for the blends mPE080 and mPE020, and for the pure components, EVAc and mPE. The following typical variables defined in the introduction for heterogeneous blends can be directly derived from these results: the relaxation time due to the interphase effects of particle deformation (τ_P), the characteristic secondary plateau (G_P) and the terminal relaxation of the blend (τ_D). As mentioned in the introduction, Palierne [6] developed a general expression for the complex shear modulus of an emulsion of undiluted viscoelastic fluids, in terms of the ratio between the interfacial tension and dispersed phase radius α/R. This model is able to describe the linear viscoelastic behaviour of heterogeneous concentrated blends over the entire range of frequencies. Under the assumption that the deformation of the inclusions remains small, and considering a constant

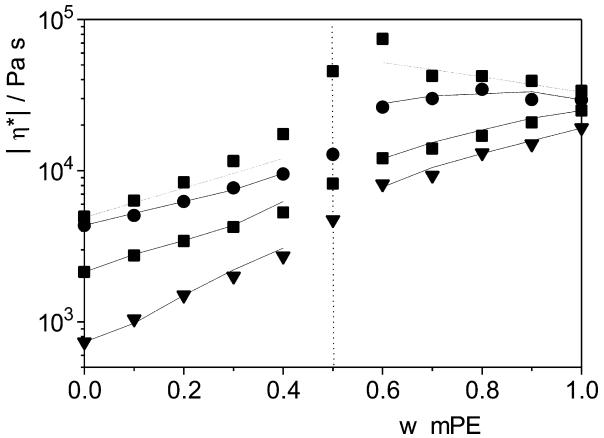

Fig. 4. Compositional dependence of viscosity at 160 °C for the blends: (■) η_0 (Maxwell fit) (●) $|\eta^*|$ ($|G^*| = 10^3$ Pa), (▲) $|\eta^*|$ ($|G^*| = 10^4$ Pa) and (▼) $|\eta^*|$ ($|G^*| = 4\times10^4$ Pa). Broken lines represent the prediction of the Oldroyd model for η_0. Continuous lines represent the prediction of the Palierne model.

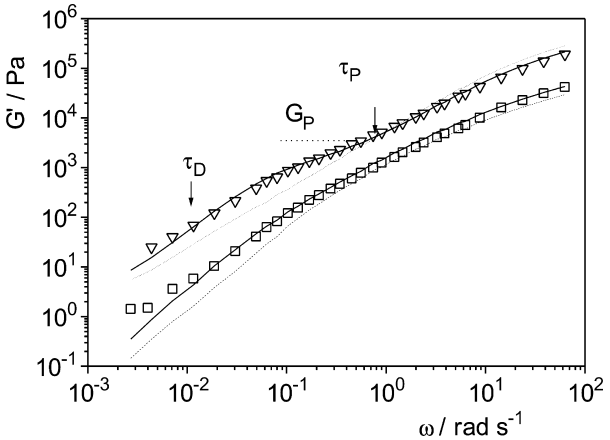

Fig. 5. Storage modulus G' versus angular frequency ω for mPE080 (▽) and mPE020 (□) blends at 160 °C. Continuous lines represent the Palierne model fit. The dashed and the dotted lines represent the behaviour of pure EVAc and mPE, respectively.

sphere particle radius R, the interfacial tension α, is the sole parameter describing the interfacial properties of the components. Owing to the lack of contrast between the components of our samples in the melt state, particle radius could not be determined. Thus, we applied the Palierne model (Eqs. (1) and (2)) to our experimental data, taking α/R as an adjustable parameter. The model provides a very good description of the linear viscoelastic response at both ends of the phase diagram (mPE080 and mPE020) with values of $\alpha/R = 3.5\times10^3$ Pa; this may be observed in Fig. 5 for the storage modulus G' and in Fig. 6, for the loss tangent tan δ. Similar behaviour (data not shown) has been observed in mPE90 and mPE10 blends. We also applied this model to the values of $|\eta^*|$ at constant $|G^*|$. It can be seen in Fig. 4 that this model provides an excellent description of the compositional dependence of this function, at least for values of $|G^*|$ higher than 10^3 Pa.

The characteristic behaviour observed for the blends of high w corresponds to that shown by heterogeneous systems

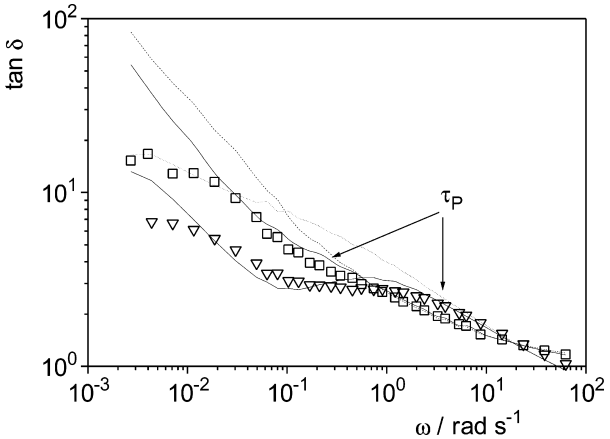

Fig. 6. Loss tangent tan δ versus angular frequency ω for mPE080 (▽) and mPE020 (□) blends at 160 °C. Continuous lines represent the Palierne model fit. The dashed and the dotted lines represent the behaviour of pure EVAc and mPE, respectively.

with a viscosity ratio between the components K lower than unity, and similar terminal relaxation times of the phases τ_m and τ_d, both within the range of the experimental time (frequency) domain [15]. For low values of w, one cannot clearly observe the characteristic variables τ_P, G_P and τ_D in G'. In this case, the system is presumably comprised of an EVAc matrix and a less deformable (more viscous) dispersed mPE phase. It follows, that the deformation mechanism that corresponds to the dispersed phase appears at lower frequencies (higher value of τ_P), the secondary plateau in G', G_P, being lower and less pronounced. Since the loss tangent is a much more sensitive viscoelastic function including both storage and loss response (tan $\times$ $\delta = G''/G'$) [28] the above effects could be more clearly observed. Indeed this is the case as shown in Fig. 6, where the relaxation mechanism is revealed by using this function.

For the intermediate compositions, the Palierne model does not fit the experimental results for G' and G'' at values of $|G^*|$ lower than 10^3 Pa, with the value of $\alpha/R = 3.5 \times 10^3$ Pa. The model does not entirely reproduce the secondary plateau zone and underestimates the storage modulus at low frequencies, as can be seen in Fig. 7. In the case of the mPE070 blend, the value of α/R (1.5×10^3 Pa) needs to be halved to obtain a good fit of the experimental data. This suggests an increase in particle radius with respect to more diluted blends (lower than $w = 0.20$ and higher than $w = 0.80$) considering that interfacial tension is a compositional independent constant (it only depends on the chemical nature of the components and slightly on temperature [29]). On the other hand, a broader plateau in G' extended at low frequencies appears for the blends of lower mPE content, as can be observed in Fig. 7. The slope of G' is sensitive to the degree of interconnectivity in materials of a network structure [30]. In dispersed morphologies, the terminal slope approaches 2 at low frequencies ($\omega < 1/\tau_d$) because the shape relaxation of the droplets ceases and the blend enters the flow terminal region. In the case of fully co-continuous morphologies, power law behaviour and lower values of the slope of G' have been observed due to the broad range in the characteristic length of domains. In our case only the blends with lower content in dispersed phase (below 30%) show slope data that approach the value of 2 exhibited by the pure EVA copolymer. However, a conspicuous decrease in the value of the slope down to 0.34 is observed for intermediate compositions. It is obvious that either experiment at very low frequency or relaxation modulus experiments could only clarify whether the characteristic power law behaviour is followed by our system. Unfortunately degradation of the samples inherent to very low frequencies and equipment limitation (one single motor drive) do not allow us to go further on the analysis of the phase behaviour.

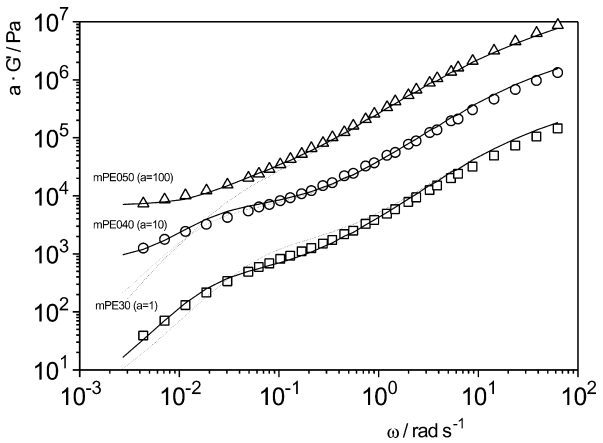

Fig. 7. Storage modulus G' versus angular frequency ω, for intermediate compositions at 160 °C. (□) mPE30, (○) mPE40 and (△) mPE050. Broken lines represent fitting to the Palierne model with variable values of α/R (3.5×10^3 Pa for MPE070 and 1.5×10^3 Pa for the rest). Continuous lines represent the fit to the modified Palierne model (see text). Please note that the true G' values are multiplied by an arbitrary constant a in order to show the three compositions in the same plot.

This power law phenomenon is not accounted for by the emulsion model. Bousmina and Muller [9] empirically modified the Palierne model by simply adding a constant value G to the storage modulus G', to take the agglomeration effect into account in thermoplastic/rubber blends, i.e. the touching among the solid particles. Dispersed liquid droplets, as it is our case, do not possibly aggregate but rather might collapse and form a co-continuous morphology with a network like behaviour (as rubber particle aggregates) showing a similar effect in G'. A suitable choice of the constant $G = 150$ *Pa* for mPE060, $G = 70$ for mPE050, $G = 20$ *Pa* for mPE040 and $G = 5$ *Pa* for mPE030 blends, gives rise to good fitting of results as one can observe in Fig. 7. These values of G would correspond to the characteristic modulus of the network structure formed by the associating deformable particles. This means that at these compositions the system presents a network-like character that should be associated to the high degree of interconnectivity among the particles [30]. Then, the maximum value of G could locate the phase inversion and a co-continuous phase formation for the composition $w = 0.60$.

The concentration at which phase inversion in immiscible blends occurs can also be determined from the rheological criteria: (i) maximum dynamic viscosity η'; (ii) maximum storage modulus G'; and (iii) minimum slope of G' [30]. In all these cases, it is necessary to gain access to the very low frequency zone. We applied all these criteria to our blends at the lowest accessible frequency and the results are shown in Table 3. It can be clearly observed that criteria (i) and (ii) locate the phase inversion composition at around $w = 0.60$ while criterion (iii) yields the lower value of $w = 0.50$. This later method, however, lacks sensitivity, given that values of the slope of G' only vary from 0.35 to 1.9 with blend composition, as was recently pointed out by Steinmann and co-workers for heterogeneous PS/PMMA blends [30]. These authors also propose that criterion (ii) is the most robust and yields a better correlation with morphological results, arguing that G' is very sensitive to morphology and morphological changes and that the

Table 3
Rheological criteria ($\omega = 0.0027$ rad s^{-1}) at a temperature of 160 °C applied to locate phase inversion composition

Sample	η' (Pa s)	G' (Pa)	G' slope
EVAc	4900	0.102	1.9
mPE010	6300	0.274	1.7
mPE020	8100	1.43	1.2
mPE030	11,100	3.69	1.1
mPE040	16,670	13.6	0.96
mPE050	25,320	62.5	0.34[a]
mPE060	54,720[a]	87.6[a]	0.67
mPE070	41,400	78.9	1.1
mPE080	40,050	17.2	1.1
mPE090	35,100	10.9	1.1
MPE	33,000	5.48	1.2

[a] These values locate the phase inversion concentration (see text for details).

criterion is more suitable for determining phase inversion concentration than for a morphological evaluation. This stems from the fact that G' reflects the three-dimensional bulk properties of the material in the melt.

Utracki [31] proposed a criterion based on Krieger and Dougherty's model for suspensions of rigid particles [32], which relies on the idea that co-continuity is associated with the maximum of viscous extra stresses. Krieger and Dougherty developed an expression for the suspension dependent upon the viscosity of the matrix η_m, the volume fraction of the second component ϕ, the maximum package fraction ϕ_M and the intrinsic viscosity $[\eta]$:

$$\eta = \eta_m\left(1 - \frac{\phi}{\phi_M}\right)^{-[\eta]\phi_M} \tag{9}$$

According to Utracki, the composition of immiscible polymer blends at which the viscosity function takes a maximum value is an isoviscous point. This point corresponds to the composition ϕ_{dI} at which adding polymer 2 to polymer 1, and viceversa, viscosity has a common value and phase inversion takes place. Accordingly, Eq. (9) gives:

$$K = \left[\frac{(\phi_M - \phi_{dI})}{\phi_M - (1 - \phi_{dI})}\right]^{-[\eta]\phi_m} \tag{10}$$

Relation (10) has been tested for a large number of immiscible blends with $[\eta] = 1.9$ and $\phi_M = 0.84$ [31]. Using this equation a value of ϕ_{dI}, 0.68, was obtained. This value was still close to those provided by means of criteria (i) and (ii). Fig. 8 shows a comparison of all the criteria defined here for predicting phase inversion in our blends. It can be observed that if one leaves out the value of 0.50 obtained from criterion (iii), the range obtained is 0.60–0.68. We think that this represents a fairly narrow range of compositions for the phase inversion mechanism.

Finally, it is worth to point out that the values of α/R obtained for the EVAc/mPE system were of the order of 10^3 Pa for all the blends and are comparable to those recorded for EVAc/LDPE blends [3] and those reported for

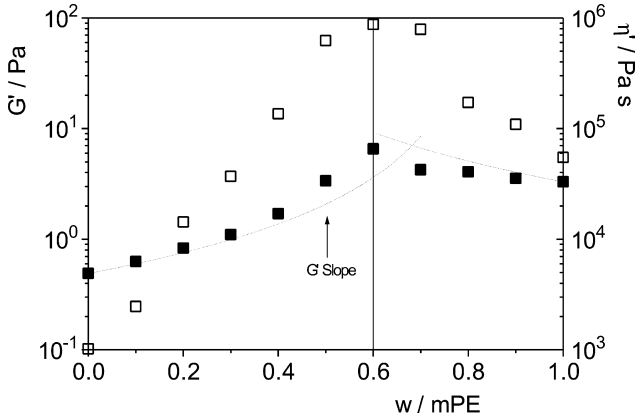

Fig. 8. Rheological criteria for predicting phase inversion composition in the blends analysed at 160 °C: (□) G' (0.0027 rad s^{-1}), (■) η' (0.0027 rad s^{-1}). The vertical continuous line represents the value of ϕ_{dI} obtained from criteria (i) and (ii). The arrow represents the value of ϕ_{dI} obtained by means of the G' slope criterion (criterion (iii)). The Broken is the blend viscosity calculated according to Eq. (10) with $\phi_M = 0.84$ and $[\eta] = 1.9$.

known heterogeneous polymer blends [26]. Owing to the lack of contrast between the two materials, we cannot foresee the morphology of the dispersed phase, but if one assumes that the size of the inclusions is of the order of 1 μm, it follows that interfacial tension will not be higher than 1 mN m^{-1} (typical values of interfacial tension for heterogeneous systems are between 0.1 and 20 mN m^{-1} at 200 °C).

4. Conclusions

Through rheological measurements, EVAc/mPE blends were found to behave as a heterogeneous polymer system. Several grades of blend morphologies were inferred by applying existing emulsion models such as the Palierne approach. These morphologies range from a phase separated dispersed system composed of viscoelastic deformable droplets of EVAc in a mPE viscoelastic matrix to a more complex structure arising from the onset of phase inversion and a probable co-continuous phase. At intermediate compositions, ca. $w = 0.60$, the generation of a three-dimensional network structure formed by the more viscous mPE surrounded by the less viscous EVAc, would explain the enhanced viscosity values observed. At lower mPE weight fractions, softening of the network structure seems to occur. Finally, a separated system of highly viscous inclusions of mPE surrounded by an EVAc matrix of lower viscosity develops. The strongest effect of phase morphology is seen in elastic properties. Intensely enhanced storage moduli were observed at low frequencies. An extended secondary plateau in the low frequency zone for blend compositions around $w = 0.60$ suggests the existence of a well developed fully co-continuous phase due to the phase inversion mechanism.

Acknowledgements

Thanks are due to the MICYT (Grant MAT2002-01242) for supporting this investigation. The authors also acknowledge Repsol-YPF Spain for their permission to publish these data.

References

[1] Zhang DD, Lee IH, Tanny SR. US 6,166,142; 2000.
[2] Fujimura T, Iwakura K. Int Chem Engng 1970;10:683.
[3] Peón J, Aguilar M, Vega JF, Del Amo B, Martínez-Salazar J. Polymer 2003;44:1589.
[4] Utracki LA. Polymer alloys and blends: thermodynamic and rheology. München: Hanser Publishers; 1989.
[5] Ajji A, Utracki LA. Polym Engng Sci 1996;36:1574.
[6] Palierne JF. Rheol Acta 1990;29:204.
[7] Graebling C, Muller R. J Rheol 1990;34:193.
[8] Graebing C, Muller R. Colloid Surf 1991;55:89.
[9] Bousmina M, Muller R. J Rheol 1993;37:663.
[10] Vinckier I, Moldenaers P, Mewis J. J Rheol 1996;40:613.
[11] Minale M, Moldenaers P, Mewis J. Macromolecules 1997;30:5470.
[12] Kitake S, Ichikawa A, Imura N, Takahashi Y, Noda I. J Rheol 1997; 41:1039.
[13] Lacroix C, Grmela M, Carreau PJ. J Rheol 1998;42:41.
[14] Yamane HM, Takahashi M, Hayashi R, Oyamoto K, Kashihara H, Masuda T. J Rheol 1998;42:567.
[15] Graebling D, Muller R, Palierne JF. Macromolecules 1993;26:320.
[16] Peón J, Vega JF, Aroca M, Martínez-Salazar J. Polymer 2001;42: 8093.
[17] Aguilar M, Vega JF, Sanz E, Martínez-Salazar J. Polymer 2001;42: 9713.
[18] Mavridis H, Shroff RN. Polym Engng Sci 1992;32:1778.
[19] van Gurp M, Palmen J. Rheol Bull 1998;67:5.
[20] Lee HS, Denn MM. Polym Engng Sci 2000;40:1132.
[21] Groves DJ, McLeish TCB, Chohan RK, Coates PD. Rheol Acta 1996; 35:481.
[22] Han CD, Yu TC. Polym Engng Sci 1972;12:71.
[23] Shih CK. Polym Engng Sci 1976;16:742.
[24] Utracki LA, Kamal MR. Polym Engng Sci 1982;22:96.
[25] Brochard F, de Gennes PG, Troain S. CR Acad Sci (Paris), Ser 2 1990; 310:1169.
[26] Hussein IA, Williams MC. Polym Engng Sci 2001;41:696.
[27] Oldroyd JG. Proc R Soc Lond, Ser A 1953;218:122.
[28] Zárraga A, Peña JJ, Muñoz ME, Santamaría A. J Polym Sci: Part B: Polym Phys 2000;38:469.
[29] Carriere C, Biresaw G, Sammler RL. Rheol Acta 2000;39:476.
[30] Steinman S, Gronski W, Friedrich C. Rheol Acta 2002;41:77.
[31] Utracki LA. J Rheol 1991;35:1615.
[32] Krieger IM, Dougherty TJ. Trans Soc Rheol 1959;3:137.